

M. D'Alessandro<sup>1,2</sup>

M. Paci<sup>1,3</sup>

A. Amadei<sup>1</sup>

<sup>1</sup> Dipartimento di Scienze e  
Tecnologie Chimiche,  
Università di Roma "Tor  
Vergata,"  
via della Ricerca Scientifica 1,  
00133 Roma, Italy

<sup>2</sup> Dipartimento di Chimica,  
Università di Roma "La  
Sapienza,"  
P.le Aldo Moro 5,  
00185 Roma, Italy

<sup>3</sup> INFM,  
sez. B,  
Rome, Italy

Received 28 January 2004;  
accepted 23 March 2004

Published online 24 May 2004 in Wiley InterScience (www.interscience.wiley.com).  
DOI 10.1002/bip.20090

## Characterization of the Conformational Behavior of Peptide Contryphan Vn: A Theoretical Study

**Abstract:** In this work we report the study of a peptide, the Contryphan Vn produced by *Conus ventricosus*, a vermivorous cone snail living in the temperate Mediterranean sea. This cyclic peptide of nine residues is a ring closed by a Cys–Cys (Cys: cysteine) disulfide bond containing two proline (Pro) residues and two tryptophans (Trp), one of them being a D-Trp. We present a statistical mechanical characterization of the peptide, simulated in water for about 200 ns with classical molecular dynamics (MD). In recent years there has been a growing interest in the study of the mechanics and dynamics of biological molecules, and in particular for proteins and peptides, about the relationship between collective motions and the active conformations which exert the biological function. To this aim we used the essential dynamics analysis on the MD trajectory and extracted, from the total fluctuations of the molecule, the dominant dynamical modes responsible of the principal conformational transitions. The Contryphan Vn small size allowed us to investigate in details the all-atoms dynamics and the corresponding thermodynamics in conformational space defined by the most significant intramolecular motions. © 2004 Wiley Periodicals, Inc. *Biopolymers* 74: 448–456, 2004

**Keywords:** molecular dynamics; conformational transitions; essential dynamics; free energy; statistical mechanics

### INTRODUCTION

In recent years, due to the growth of computer power as well as to the development of sophisticated theoretical models, a systematic study of highly complex systems like biomolecules has become affordable.

However, a quantitative complete characterization of macromolecules, such as proteins in solution, requires a computational effort that is still prohibitive; on the other hand, peptides may be now completely characterized at a reasonable computational cost. In this work we study the 9-residue Contryphan Vn peptide,

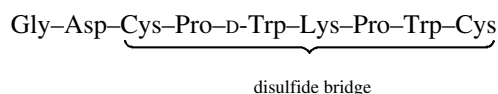
Correspondence to: andrea.amadei@uniroma2.it

*Biopolymers*, Vol. 74, 448–456 (2004)

© 2004 Wiley Periodicals, Inc.

in water, using long ( $\approx 200$  ns) classical molecular dynamics (MD) simulations. The isolation, purification, and biochemical characterization of Contryphan Vn, extracted from the venom of *Conus ventricosus*, has been recently obtained.<sup>1,2</sup> Contryphan Vn is the first conopeptide of the Contryphan family for which a pharmacological target is known. As has been recently demonstrated, it modulates the activity of  $\text{Ca}^{2+}$ -dependent  $\text{K}^+$  channels in insect neurosecretory cells and rat fetal chromaffin cells.<sup>2</sup>

The amino acid sequence of Contryphan Vn is reported below:



where the C-terminal is amidated.

Very recently, the solution structure of Contryphan Vn has been determined by NMR spectroscopy, using a variety of homonuclear and heteronuclear NMR methods and restrained MD simulations.<sup>3</sup> As already found in other contryphanes, one of the two prolines, the *cis* Pro4, may undergo a *cis-trans* isomerization while Pro7 is completely stable in its *trans* configuration. Moreover, a persistent salt bridge between Asp2 (Asp: aspartate) and Lys6 (Lys: lysine) was also revealed by the diagnostic observation of specific nuclear Overhauser effects (NOEs).

Finally, the NMR study evidenced that the contryphan structural motif represents a robust and conserved molecular scaffold whose main structural determinants are the size of the intercysteine loop and the presence and location in the sequence of the D-Trp and the two Pro residues.

A highly detailed theoretical characterization of the peptide is hence extremely useful to elucidate the structural and dynamical features as well as the thermodynamics of Contryphan Vn.

From our results it turns out that the dynamics of the side chains provides the main conformational fluctuations, while the backbone is indeed rather rigid and hence is less important in determining the global motion of the molecule.

The MD trajectories, analyzed with the Essential Dynamics analysis<sup>4</sup> reveal the presence of a few dominant concerted motions, mainly related to the conformational transitions of the side chains of the two tryptophans.

With these collective degrees of freedom, it is possible to evaluate the free energy surface of the dominant conformational transitions at two different temperatures (300 and 400 K), and to pinpoint the

relationship between these essential degrees of freedom and the structural features of the peptide.

## METHODS

The starting coordinates of Contryphan Vn were obtained from those of R-contryphan, taken from the Protein Data Bank<sup>5,6</sup> and by manually performing the mutations of different residues. The very recent determination of Contryphan Vn structure<sup>3</sup> has confirmed its high similarity to R-contryphan structure.

The molecule was immersed in a rectangular box, with sides aligned along its principal axis, filled with 429 SPC water molecules<sup>7</sup> and 1 chloride ion, introduced to retain a neutral system. Nonpolar hydrogen atoms were not included in the calculation, while all other atoms were explicitly treated.

Before starting the productive simulation, the system was prepared with a multiple step procedure. First, we performed a steepest descent minimization followed by a MD equilibration of the water with the contryphan atoms fixed. Subsequently, a steepest descent minimization of the whole system was performed. Finally, many short MD simulations (20 ps) of the whole system from  $T=50$  K to 300 K and, as a final step, an equilibration MD run of 1.4 ns, at the desired temperature, were done.

Simulations were performed according to NVT ensemble, keeping the temperature fixed with the Iso-Gaussian thermostat.<sup>8</sup> This was done in order to obtain results fully consistent with statistical mechanics.<sup>9,10</sup>

Bond lengths were constrained using the Lincs procedure,<sup>11</sup> nonbonded short-range interactions were evaluated using a cutoff of 0.9 nm and the time step was 2 fs.

The electrostatic long-range interactions were evaluated through the Particle Mesh Ewald summation method,<sup>12</sup> with a fourth-order cubic interpolation.

The time length of the productive simulation was 210 ns at  $T=300$  K and 190 ns at  $T=400$  K. MD simulations were performed with the parallel version of GROMACS,<sup>13-15</sup> modified for the removal of the peptide translational and rotational motions,<sup>9</sup> thus obtaining only the internal motions of the molecule.

The trajectories were analyzed extracting the essential degrees of freedom according to the method of the Essential Dynamics Analysis.<sup>4</sup> This method, equivalent to a principal component analysis on the coordinate fluctuations<sup>16</sup> and related to quasi-harmonic analysis,<sup>17</sup> has been shown to be a very useful tool to identify the main protein internal motions, and has been successfully applied to describe the behavior of several proteins.<sup>18-22</sup>

This method allows a separation of the configurational space into two subspaces: an essential one of very low dimensionality, which is responsible for the main part of the positional fluctuations, and the remaining high dimensional one, characterized by nearly constrained gaussian-like fluctuations.

Diagonalizing the covariance matrix  $C$  of the atomic fluctuations provides a set of eigenvectors and eigenvalues.

$$C = \langle (\mathbf{x} - \langle \mathbf{x} \rangle)(\mathbf{x} - \langle \mathbf{x} \rangle)^T \rangle$$

The eigenvalues can be sorted in decreasing order and the essential degrees of freedom are identified by the eigenvectors associated to the largest eigenvalues.

The eigenvalues are the averaged squared fluctuations in configurational space along the corresponding directions of the motion (the eigenvectors), and their sum provides a measure for the amount of the sampled configurational phase space.

$$\sum_i (x_i - \langle x_i \rangle)^2 = \sum_i \lambda_i$$

## RESULTS

### Convergence Analysis

The noise in the covariance matrix definition, and as a consequence, in its eigenvectors, is due to the insufficient configurational space sampling of finite length simulations: the Covariance matrix we compute, is an estimate of the infinite-time one. The accuracy of this estimate depends on the accuracy of the phase space sampling. Hence, we will expect that the eigenvectors should converge to the asymptotic ones for long enough trajectories. In this subsection, as a first point, we study, in quantitative details, the convergence of the eigenvectors in time, using pairs of independent trajectories of increasing time length. This is done by computing the root mean squared inner product (RMSIP)<sup>23</sup>:

$$\text{RMSIP} = \left( \frac{1}{10} \sum_{i=1}^{10} \sum_{j=1}^{10} (\boldsymbol{\eta}_i \cdot \boldsymbol{\nu}_j)^2 \right)^{1/2}$$

between the eigenvectors  $\boldsymbol{\eta}$  and  $\boldsymbol{\nu}$  of subparts of the trajectory of increasing time length (one taken from the beginning and one from the end in order to prevent any dynamical correlation); the sum is restricted to 10 since we consider the essential subspace as defined by the first 10 eigenvectors associated with the largest eigenvalues.

From the definition it comes out that the higher the RMSIP ( $\leq 1$ ), the better the convergence. If RMSIP=1, the subspace spanned by the two different sets of eigenvectors would coincide.

In Figure 1 it is shown the RMSIP, from all atom eigenvectors, up to 50 ns for both the simulations at 300 K and 400 K. It is evident that a significant

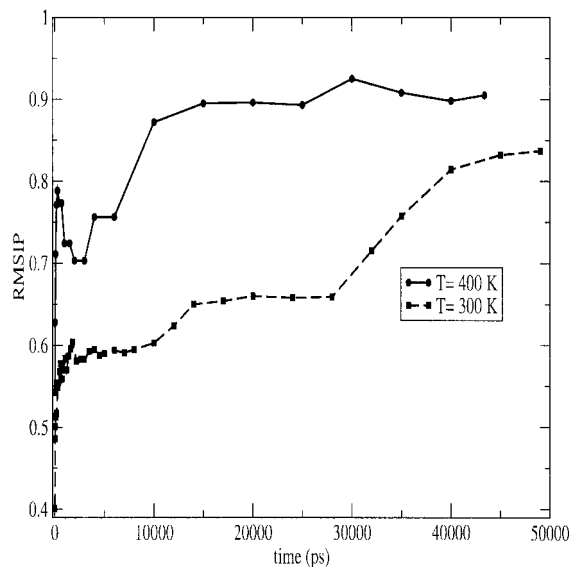


**FIGURE 1** RMSIP vs time, for the simulation at  $T=300$  K (dashed line) and  $T=400$  K (solid line).

convergence is reached in the very beginning of the simulation, while a slower further convergence is obtained afterwards. Moreover, the simulation at 300 K requires much longer time to reach a very good convergence of the essential ten-dimensional subspace with respect to the simulation at 400 K.

Nevertheless, the final overlap between the conformational subspaces (over about 100 ns) is quite high and similar for both simulations: 0.88 at 300 K and 0.89 at 400 K.

We also analyzed the RMSIP for the backbone eigenvectors, finding a considerable convergence of the essential subspace (e.g., 0.78 at 300 K) within a few nanoseconds. This faster convergence causes the choice, usual for larger molecules, of restricting the analysis to the backbone atoms.

Since the essential subspaces at the two different temperatures define the main dynamical and structural transitions of Contryphan Vn, it should be interesting to analyze the overlap of the essential subspaces at the two different temperatures. In this case the RMSIP computed from the whole trajectories reaches the value of 0.91, thus revealing that the essential ten-dimensional subspace is quite conserved from 300 to 400 K.

In order to evaluate the statistical significance of the observed overlaps of the eigenvectors, we performed a statistical assessment, for both temperatures, on the eigenvectors obtained from the two halves of the trajectories, according to the method described in a previous article.<sup>23</sup> In such a statistical analysis the inner product distribution of one eigenvector set onto

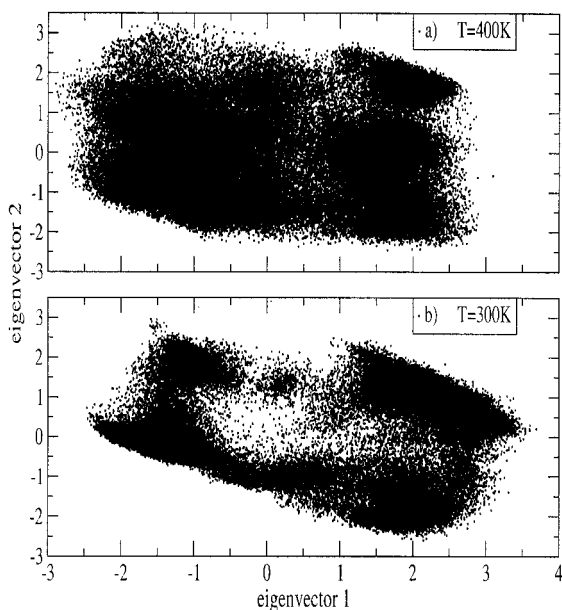


**FIGURE 2** Projections of the trajectories onto their own first eigenvector plane at  $T=400$  K (a) and  $T=300$  K (b).

another is compared with the inner product distribution of a random vector onto a fixed basis set. The two eigenvector sets are considered statistically similar when their overlap is higher than that obtained from the random distribution at a given statistical confidence threshold (in our case 99%). The results revealed that the eigenvectors are significantly converged, and hence, may be a statistically reliable approximation of the infinite-time ones.

Interestingly, from the same assessment it is found that the first two-dimensional planes of 300 and 400 K exhibit a statistically significant overlap, implying that the increase of the temperature basically provides a simple rotation of the eigenvectors in the same plane.

Moreover, the observed good convergence of the eigenvectors at each temperature implies a rather dense sampling of configurational space, clearly due to the use of an extended MD trajectory (200 ns). In fact, although a time scale of a few nanoseconds allows the separation between essential and nearly constrained subspaces, the essential one remains poorly filled in by the trajectory.<sup>23</sup> The dense sampling that we obtain is illustrated by the projections of the trajectories at  $T=300$  and 400 K onto their own first essential two-dimensional plane (Figure 2). At  $T=400$  K it is evident a quite uniform density, with just a weaker spot between 0 and 1 along the first eigenvector. This can suggest the presence of a relatively low free energy barrier between two different stable conformations along this eigenvector.

At  $T=300$  K the situation is different: we can observe some different dense spots, whereas other regions are clearly not easily accessible by the system, hence suggesting the presence of a few stable conformations separated by high free energy barriers.

## Structural Motions

In this subsection, we will show in details the results of the Essential Dynamics analysis of Contryphan. As the molecule is constituted of 102 atoms, the diagonalization of the covariance matrix gives a set of 306 eigenvectors and eigenvalues. Among all these, as observed in other molecules,<sup>18, 24–26</sup> only a small fraction is typically associated with significant fluctuations, i.e., eigenvalues significantly different from zero. These essential eigenvectors are responsible for the main internal motions of the molecule, the others behaving in a nearly constrained way with usually gaussian-like distributions and almost null eigenvalues; moreover, six eigenvalues must be virtually zero as associated with holonomic constraints (rototranslational constraints).

In Figure 3 the first 100 eigenvalues are reported. Interestingly, even if the total conformational fluctuation, i.e., the sum of all the eigenvalues, is higher at  $T=400$  K, the first eigenvalue at 300 K is the highest one. This is due to the 300 K anisotropic distribution of Figure 2, which provides a low density close to the average structure (central part of the figure).

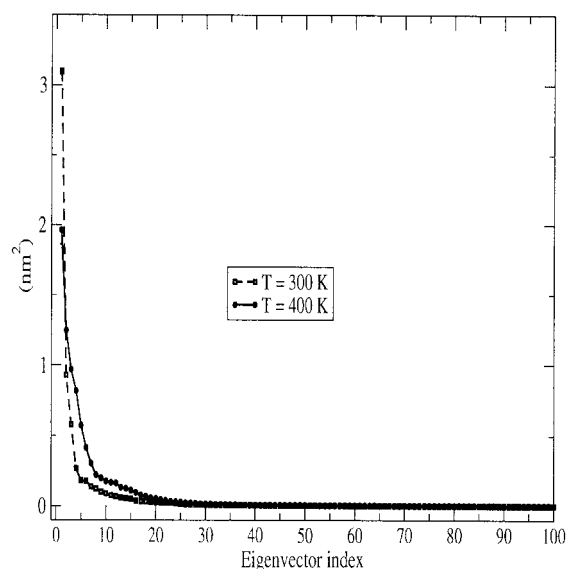


**FIGURE 3** Eigenvalues of the covariance matrix from the simulations at  $T=300$  K (dashed line) and  $T=400$  K (solid line).

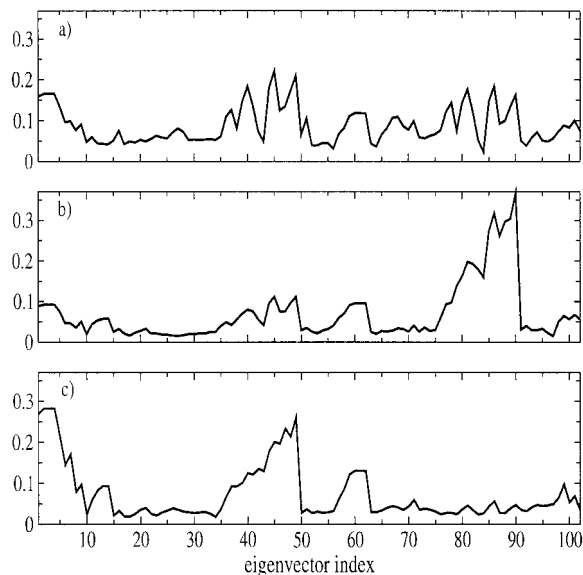


**FIGURE 4** Atom composition of eigenvector 1 (a), 2 (b), and 3 (c), from the simulation at  $T=300$  K.

In order to understand the configurational meaning of the essential eigenvectors, the atom components of the first three eigenvectors are shown (Figures 4 and 5) as well as the projection of the trajectory onto them (Figure 6).

We just remind the sequence of Contryphan's amino acidic residues with the atom index below (see Table I).

From Fig. 4 it turns out that at  $T=300$  K the concerted motion, associated to the first eigenvector,

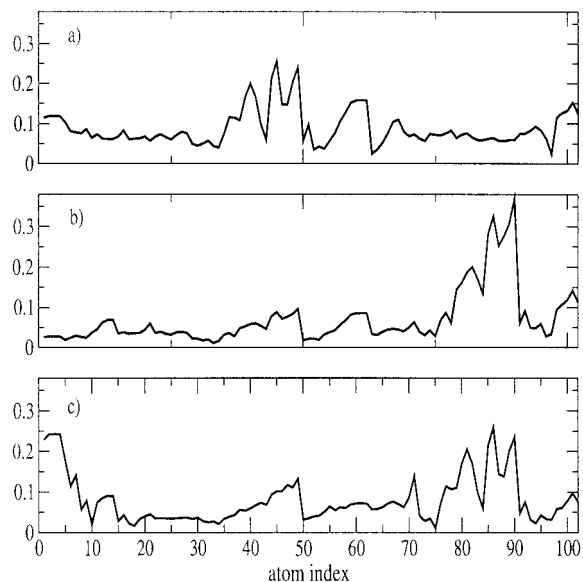


**FIGURE 5** Atom composition of eigenvector 1 (a), 2 (b), and 3 (c), from the simulation at  $T=400$  K.

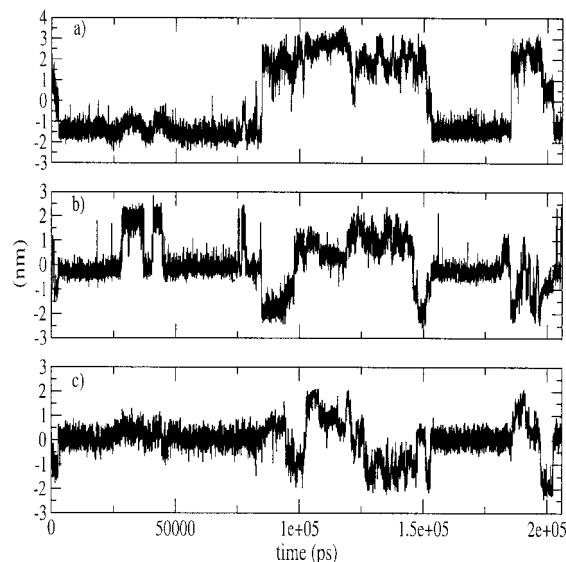


**FIGURE 6** Projection of the trajectory at  $T=300$  K onto eigenvector 1 (a), 2 (b), and 3 (c).

is mainly composed of atoms belonging to D-Trp5, Trp8, Gly1 (Gly: glycine), and Lys6; the second mainly of atoms belonging to Trp8 and the third to Gly1, D-Trp5, and Lys6.

The same four residues are involved in the first three eigenvectors at  $T=400$  K, as shown in Figure 5, but a minor coupling of these residues is present: the first eigenvector has components mainly in D-Trp5 and Lys6, the second in Trp8 and the third in Gly1. This result agrees well with the previous finding of the rotation of the eigenvectors defining the first two-dimensional-essential subspace, when raising the temperature from 300 to 400 K.

Moreover, from Figures 4 and 5 it is evident the main role of the two tryptophans in the structural fluctuations of the whole peptide, with the coordinated motion of Gly1 and Lys6. In particular, the existence of coordinated motions of Trp8 and Lys6 is in agreement with some experimental evidence<sup>1</sup> of a stable 6 Å distance between this two residues, similar to those observed in several toxins binding potassium channels.

The eigenvectors obtained from the diagonalization of the covariance matrix of the backbone fluctuations at  $T=300$  K reveal that D-Trp5, Lys6, and Trp8 are all totally absent from the first three essential eigenvectors, which have components mainly in Gly1 (data not shown). The comparison of the behavior for the all-atoms and the backbone eigenvectors shows that the main structural fluctuations of this peptide reside in the side chains motions, as expected from the presence of the D-Trp and the disulfide bond. This is

**Table I** Sequence of Contryphan Vn Residues with the Corresponding Atom Index

Gly1	Asp2	Cys3	Pro4	D-Trp5	Lys6	Pro7	Trp8	Cys9
1–7	8–16	17–23	24–30	31–51	52–64	65–71	72–92	93–102

also confirmed by observing that the total fluctuation of the backbone is much lower than that of all atoms.

The projection of the 300 K trajectory onto the first essential eigenvector (Figure 6) shows a two-state behavior, which can be related with the fluctuation of the side chains of the Trp's and Lys. Only a few transitions occur during the simulation as the permanence in each stable state takes very long times. At 400 K the two state behavior is also evident in the first eigenvector, but with a ten-time increased frequency for the transitions.

### Free Energy Calculations

The results shown so far clearly indicate the main importance, in the Contryphan Vn dynamical behavior, of a few residues and reveal the presence of a limited set of long-life conformational states, thus pointing out the existence of a multiple free energy minima landscape.

In this section we describe the free energy surface evaluated in the plane defined by the first two essential eigenvectors, defining the main two conformational coordinates of the peptide.

In order to do this, a grid is constructed and the density of configurations in each cell of the grid is computed. The Helmholtz free energy surface is obtained via the probability distribution ( $P_{i,j}$ ),

$$A_{i,j} - A_{0,0} = -RT \ln(P_{i,j}/P_{0,0})$$

where  $R$  is the ideal gas constant,  $T$  is the actual temperature, and  $i,j$  are respectively the row and column index of the grid cell, with  $P_{0,0}$  and  $A_{0,0}$  the probability of a reference grid cell and the corresponding free energy.

To obtain the free energy curve along the first essential eigenvector, we must sum  $P_{i,j}$  on one index:  $P_i = \sum_j P_{i,j}$ ,  $P_0 = \sum_j P_{0,j}$ , and  $A_i - A_0 = -RT \ln(P_i/P_0)$ . In Figure 7 the three curves correspond to the free energies calculated from the 300 K simulation along its own first eigenvector and from the 400 K simulation along both 300 and 400 K first eigenvectors.

It is worth noting that at  $T = 300$  K two well-defined minima exist (corresponding to the stable states shown in Figure 6). Between the two minima a free energy barrier of about 10 KJ/mole is present,

which explains the low frequency of the conformational transitions. The free energy curve for 400 K simulation as a function of the position along the first 300 K eigenvector still exhibits the two minima, even if they are significantly raised (with a corresponding barrier, of less than 3 KJ/mole), and slightly shifted with respect to the 300 K ones. Interestingly, the curve of the 400 K simulation on its own first eigenvector exhibits the two minima at the same positions of the 300 K one, although with a rather lower barrier of about 5 KJ/mole.

These results are in agreement with our previous finding about the rotation of the essential eigenvectors when the temperature is increased. The first 300 K eigenvector is essentially a superposition of the first two 400 K eigenvectors. Moreover, since the free energy barrier, at 400 K, is comparable to the thermal energy (3.32 KJ/mole), the conformational transition can occur at much higher frequency, as indeed observed in the simulation.

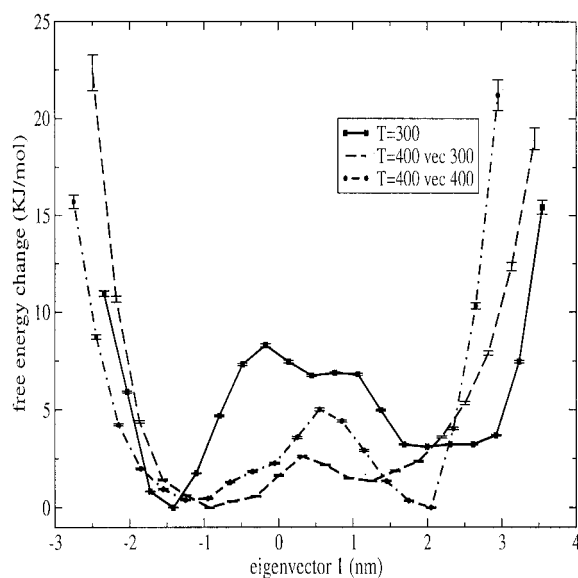


**FIGURE 7** One-dimensional Helmholtz free energy pattern projected onto the first eigenvector: the solid line is obtained from the simulation at  $T=300$  K onto its own first eigenvector, the dashed line is obtained from the simulation at  $T=400$  K onto the 300 K first eigenvector, and the dot-dashed line is obtained from the simulation at  $T=400$  K onto its own first eigenvector.

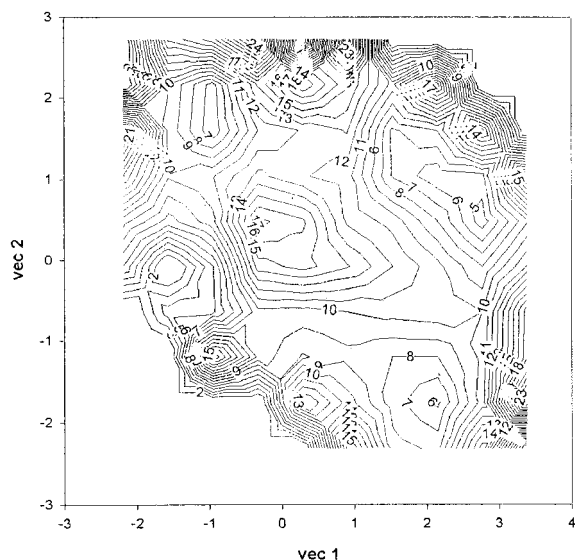


**FIGURE 8** Two-dimensional Helmholtz free energy (KJ/mol) at  $T=300$  K surface projected onto its own first eigenvector plane.

The contour plot at  $T=300$  K allows a more detailed overview of the free energy landscape, showing a more complex situation (Figure 8).

Interestingly, from this figure it is clear that the deeper and narrower free energy minimum of Figure 7 correspond to the deepest and narrowest minimum in Figure 8, while the other free energy minimum of Figure 7 is actually a combination of two different higher and broader minima in Figure 8. Moreover, many other less significant minima are present in the surface.

From the definition of the first eigenvector and the peptide structure at the free energy minima and maximum of Figure 7, it emerges that the two free energy minima correspond to configurations where Trp hydrophobic side chains are in proximity of the peptide backbone, while in the configurations of the free energy maximum the two Trp side chains are exposed to

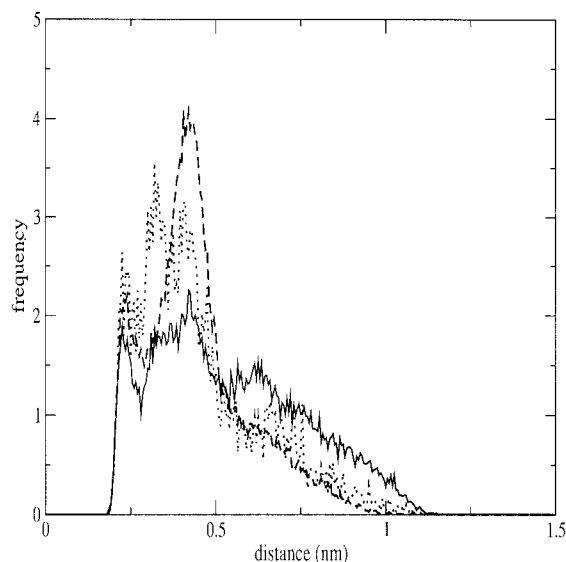


**FIGURE 10** Histogram of the salt bridge between Asp2 and Lys6 computed from configurations extracted in the absolute minimum (dashed line), maximum (dotted line), relative minimum (solid line) of the free energy curve at 300 K.

the solvent. This is indeed shown in Figure 9, where three peptide structures corresponding to the free energy minima (panels a and c) and maximum (panel b) for the 300 K first eigenvector are reported.

From our simulation data we can also monitor the stability of the experimentally evidenced salt bridge between Asp2 and Lys6 and its relation with the free energy pattern along the first essential eigenvector. The analysis of the distance between Asp2 and Lys6 side chains definitely reveals a persistent salt bridge (distance  $\leq 5\text{\AA}$ ), as shown in Figure 10, which is particularly favored in the deepest free energy minimum.

Moreover, the dynamical behavior of proline 7, unlike proline 4, is influenced by the free energy pattern along the first eigenvector, as clearly shown

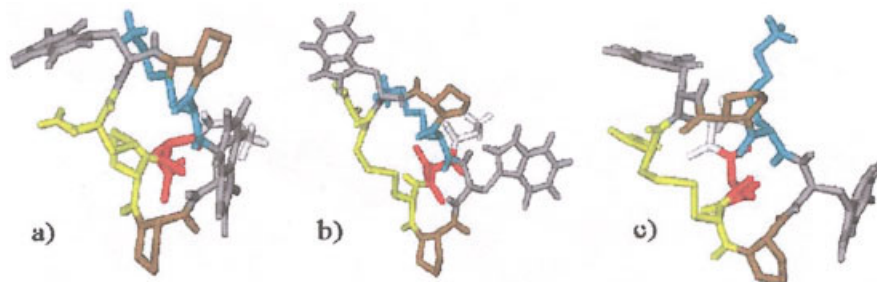


**FIGURE 9** Structures corresponding to free energy absolute minimum (panel a), maximum (panel b), and relative minimum (panel c).

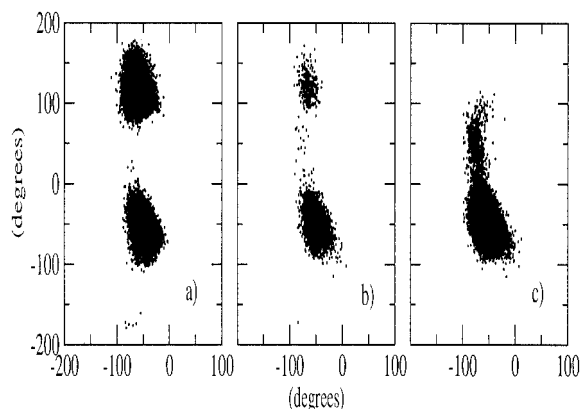


**FIGURE 11** Ramachandran plot of Pro7 computed from configurations extracted in the (a) absolute minimum, (b) maximum, and (c) relative minimum of the free energy curve at 300 K.

by the Ramachandran plot at 300 K (Figure 11). In Figure 12 we show the time dependence of the improper dihedral angle for these two residues. It must be noted that this is the angle between the planes  $C-N-C_\alpha$  and  $C-C_\delta-C_\alpha$ , where C is the carbonyl carbon atom. Such an angle may provide a suitable property for monitoring the attempt of each proline to undergo the *cis-trans* isomerization, although complete isomerization cannot occur in a MD simulation where the force field defines the *cis* or *trans* proline configuration. From the figure it is evident that proline 4 has a much wider range of angle fluctuations, suggesting its attempt to isomerize from *cis* to *trans*. Such a result is also evidenced by Figure 13, where

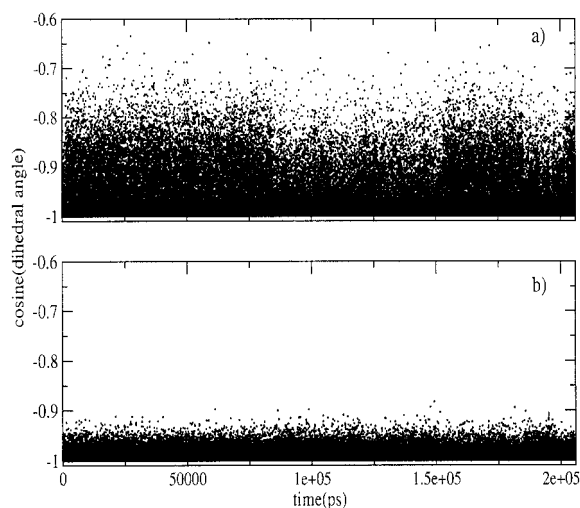


**FIGURE 12** Cosine of the dihedral angle (interesting for monitoring the attempt of each proline to undergo the *cis-trans* isomerization) vs time, for Pro4 (a) and Pro7 (b).

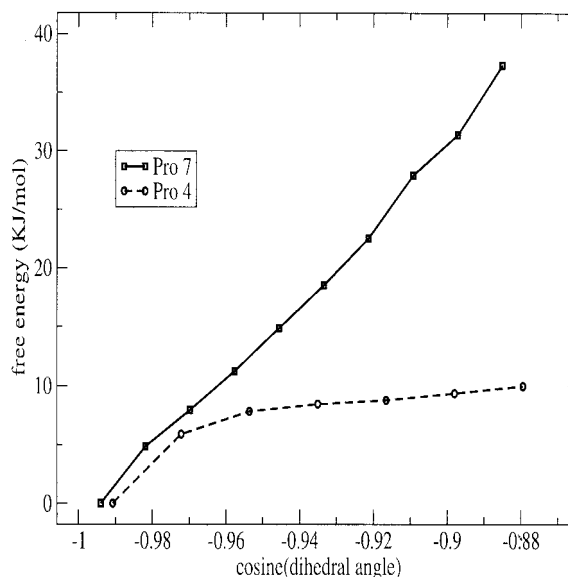


**FIGURE 13** Free energy pattern for the Pro4 (dashed line) and Pro7 (solid line) as a function of the cosine of the dihedral angle.

the free energy profiles as a function of the improper dihedral is shown for the two prolines. This figure clearly indicates that, while for proline 7 there is a high free energy barrier for the *trans-cis* isomerization, in the case of proline 4 a flatter free energy is associated with the same transition, in agreement with the previously mentioned recent NMR results.<sup>3</sup>

## CONCLUSIONS

The results reported in this article show that the combined use of MD simulations and theoretical analysis gives a rather complete and accurate description of a biochemical molecular system such as a solvated peptide.

From the Essential Dynamics analysis we find that the main structural fluctuations of the peptide reside mainly in the concerted motions of the tryptophans side chains, while the backbone shows a reduced flexibility (this could be expected because of the strong constrain due to the disulfide bridge between the two cysteines).

The conformational transition defined by the first eigenvector (the dominant concerted motion) can be related to a well-defined free energy landscape, showing the existence of low free energy states separated, at 300 K, by high-energy barriers.

Interestingly, simulation data show the presence of a stable salt bridge between Asp2 and Lys6 and a

possible *cis-trans* isomerization only for proline 4, in agreement with NMR results.

The Italian ministry of University and Research (MIUR) is acknowledged for funding by FIRB projects.

Paolo Ascenzi and Fabio Polticelli are gratefully acknowledged for discussions and interest in the study of contryphans; Daniel O. Cicero and Tommaso Eliseo are gratefully acknowledged for helpful discussions of our results with respects to NMR data. Alfredo Di Nola is gratefully acknowledged for encouraging to extend simulations to miniproteins.

## REFERENCES

1. Raybaudi Massilia, G.; Schininà, M. E.; Ascenzi, P.; Polticelli, F. *Biochem Biophys Res Comm* 2001, 288, 908.
2. Raybaudi Massilia, G.; Eliseo, T.; Grolleau, F.; Lapied, B.; Barbier, J.; Bornaud, R.; Molgo, J.; Cicero, D. O.; Paci, M.; Schininà, M. E.; Ascenzi, P.; Polticelli, F. *Biochem Biophys Res Comm*. 2003, 303, 238.
3. Eliseo, T.; Cicero, D. O.; Romero, C.; Schininà, M. E.; Raybaudi Massilia, G.; Polticelli, F.; Ascenzi, P.; Paci, M. *Biopolymers*, in press.
4. Amadei, A.; Linssen, A. B. M.; Berendsen, H. J. C. *Proteins Struct Funct Genet* 1993, 17, 412.
5. Protein Data Bank, 1999, [www.rcsb.org/pdb](http://www.rcsb.org/pdb); code: 1QFB.
6. Pallaghy, P.; Melnikova, A.; Jimenez, E. C.; Olivera, B. M.; Norton, R. S. *Biochemistry* 1999, 38, 11559.
7. Berendsen, H. J. C.; Postma, J. P. M.; van Gunsteren, W. F.; Hermans, J. *Intermolecular Forces*; Pullmann, B., Ed.; D. Reider Publishing Company: Dordrecht, 1981; p 331.
8. Evans, D. J.; Morris, G. P. *Phys Lett* 1983, 98A, 433.
9. Amadei, A.; Chillemi, G.; Ceruso, M. A.; Grottesi, A.; Di Nola, A. *J Chem Phys* 2000, 112, 9.
10. D'Alessandro, M.; Tenenbaum, A.; Amadei, A. *J Phys Chem B* 2002, 106, 5050.
11. Hess, H.; Bekker, B.; Berendsen, H. J. C.; Fraije, J. G. E. M. *J Comp Chem* 1997, 18, 1463.
12. Darden, T.; York, D.; Pedersen, L. *J Chem Phys* 1993, 98, 12, 10089.
13. van der Spoel, D.; van Drunen, R.; Berendsen, H. J. C. GRoningen MACHine for Chemical Simulations, Department of Biophysical Chemistry, BIOSON Research Institute, Nijenborgh 4 NL-9717 AG Groningen, 1994; email: [gromacs@chem.rug.nl](mailto:gromacs@chem.rug.nl).
14. van der Spoel, D.; van Buuren, A. R.; Apol, E.; Meulenhoff, P. J.; Tieleman, D. P.; Sijbers, A. L. T. M.; van Drunen, R.; Berendsen, H. J. C. *Gromacs User Manual Version 1.3*, Nijenborgh 4, 9747 AG Groningen, The Netherlands, 1996; Internet: <http://rugmd0.chem.rug.nl>.
15. van Gunsteren, W. F.; Billeter, S. R.; Eising, A. A.; Hunenberger, P. H.; Kruger, P.; Mark, A. E.; Scott, W. R. P.; Tironi, I. G. *Biomolecular Simulation: The GROMOS96 Manual and User Guide*; Hochschulverlag AG an der ETH Zurich: Zurich, 1996.
16. Garcia, A. E. *Phys Rev Lett* 1992, 68, 2696.
17. Ichyue, T.; Karplus, M. *Proteins Struct Funct Genet* 1991, 11, 205.
18. de Groot, B. L.; van Aalten, D. M. F.; Amadei, A.; Berendsen, H. J. C. *Biophys J* 1996, 71, 1707.
19. Pang, A.; Arinaminpathy, Y.; Sansom, M. S. P.; Biggin, P. C. *Febs Letters* 2003, 550, 168.
20. A.; Grottesi and M. S. P. Sansom, *Febs Letters* 2002, 535, 29.
21. Daidone, I.; Amadei, A.; Roccatano, D.; Di Nola, A. *Biophys J* 2003, 85, 2865.
22. de Groot, B. L.; Daura, X.; Mark, A. E.; Grubmuller, H. *J Mol Biol* 2001, 309, 299.
23. Amadei, A.; Ceruso, M. A.; Di Nola, A. *Proteins Struct Funct Genet* 1999, 36, 419.
24. de Groot, B. L.; van Aalten, D. M. F.; Scheek, R. M.; Amadei, A.; Vriend, G.; Berendsen, H. J. C. *Proteins Struct Funct Genet* 1997, 29, 240.
25. de Groot, B. L.; Hayward, S.; van Aalten, D. M. F.; Amadei, A.; Berendsen, H. J. C. *Proteins Struct Funct Genet* 1998, 31, 116.
26. Chillemi, G.; Falconi, M.; Amadei, A.; Zimatore, G.; Desideri, A.; Di Nola, A. *Biophys J* 1997, 73, 1007.

*Reviewing Editor: Dr. J. Andrew McCammon*